

# Use of bacterial cellulose film modified by polypyrrole/TiO<sub>2</sub>-Ag nanocomposite for detecting and measuring the growth of pathogenic bacteria



Samaneh Ghasemi<sup>a</sup>, Mahmoud Rezazadeh Bari<sup>a</sup>, Sajad Pirsaa<sup>a,\*</sup>, Saber Amiri<sup>b</sup>

<sup>a</sup> Department of Food Science and Technology, Faculty of Agriculture, Urmia University, P.O. Box 57561-51818, Urmia, Iran

<sup>b</sup> Department of Food Science and Technology, Faculty of Agriculture, University of Tabriz, Tabriz, Iran

## ARTICLE INFO

### Keywords:

Bacterial cellulose  
Polypyrrole  
TiO<sub>2</sub>-Ag  
Nanocomposite  
Biosensor

## ABSTRACT

The aim of this study was to use of bacterial cellulose/polypyrrole/TiO<sub>2</sub>-Ag (BC/PPy/TiO<sub>2</sub>-Ag) nanocomposite film to detect and measure the growth of 5 pathogenic bacteria. For this purpose, at first, 13 BC/PPy/TiO<sub>2</sub>-Ag films were fabricated, then bacterial suspensions were prepared according to McFarland standard. The results showed that by increasing the bacterial concentration, the electrical resistance of sensors was decreased and there was a relation between bacterial concentration and bacterial type with electrical resistance change of sensors. The obtained data showed that the sensitivity of the sensors was increased with increasing the concentration of polypyrrole and TiO<sub>2</sub>-Ag. FT-IR and SEM tests were performed to investigate the interaction between nanoparticles and determine the size of nanoparticles. The BC/PPy/TiO<sub>2</sub>-Ag biosensors are portable and the response time of these sensors is very short for target analysis. Therefore, these sensors have the potential to improve biological safety as diagnostic tools.

## 1. Introduction

Assessing the level of bacterial contamination in the production process is one of the major problems in the food and drink industry because the outbreak of harmful bacteria is considered a risk to the health of the consumer (Hamada et al., 2013). Increased concerns about the microbiological safety of food, water, dairy products, industrial waste and pharmaceutical products have required the development of reliable methods for detecting contaminants (DaSilva, Oliveira, de Melo, & Andrade, 2014).

In the food industry, the rapid production is very important, also the quality control of products is very important. In recent years, rapid and automatic methods in food microbiology have been emphasized to measure microbial count. In order to estimate the number of microorganisms according to their metabolism, there are different methods that are widely used in the food industry, including food insecure control, food preservatives control, food fermentation control, and control of food pathogens (Yang & Bashir, 2008). Colony counting, immunological methods such as enzyme-linked immunosorbent assay (ELISA) and nucleic acid-based methods such as polymerase chain reaction (PCR) are commonly used methods to identify bacteria. The colony counting method is a time consuming method. Immunological

methods require expensive laboratory materials as well as several washing steps. Nucleic acid-based methods are expensive and require specialized facilities. Although these methods are sufficiently sensitive and selective, but cost-effectiveness and complexity of these methods are disadvantages of them (Wan, Sun, Qi, Wang, & Zhang, 2014). The rapid identification of pathogen bacteria is very important in many health and safety fields including medicine, food industry and the environment (Yoo, Kim, & Lee, 2015). Therefore, it is essential to develop affordable and reliable tools that allow rapid, selective, and high-sensitivity analysis. As a result, humans can have a healthier and more reliable life. Therefore, the use of biosensors has become popular in recent years (Hiremath, Guntupalli, Vodyanoy, Chin, & Park, 2015). Biosensors are emerging technologies that are capable of achieving fast results. In addition to high-speed action, these sensors are very sensitive (Wang & Alocilja, 2015). Among the biosensors, the electrochemical biosensors have become an attractive tool for being low cost, fast response, ease of operation, high sensitivity and selectivity. Recent studies have shown that there is a growing interest in developing biosensors as a quick and accurate approach to detecting food pathogens. In recent years, the development of sensors using nanomaterials and the use of nanotechnology has been developed. Nanomaterials have improved the sensor detection capability. Nanoscale materials have

\* Corresponding author.

E-mail address: [s.pirsaa@urmia.ac.ir](mailto:s.pirsaa@urmia.ac.ir) (S. Pirsaa).

attracted considerable attention from the scientific community due to their unique properties (Detsri & Popanyasak, 2015). Advantages of using biosensors in the food industry include the ability to identify a specific composition, relatively low cost of production compared to other methods, small size production, simple operation and portability (Luong, Mulchandani, & Guilbault, 1988). One of the most important uses of biosensors in the food industry is the detection of contamination in raw food and the control of fermented products (Panfili, Manzi, Compagnone, Scarciglia, & Palleschi, 2000). The general principles of conducting-biosensors are change in conductivity due to the change in the concentration of microorganisms on the electrode surface (Lei, Chen, & Mulchandani, 2006). Conducting polymers have attracted considerable attention as applied materials due to their unique electrical features and controllable chemical and electrochemical properties. Polypyrrole, polythiophene, polyacetylene, polyaniline and poly-*paraphenylene* are conducting polymers that are used commonly in different fields. Polypyrrole (PPy) has attracted the attention of many researchers as one of the most important conductive polymers. The features of this polymer, such as the convenience of its preparation and synthesis, environmental stability and high conductivity cause to its use in various fields, such as the construction of sensors and electrical instruments. Bacterial cellulose is a microbial polysaccharide that has unique properties that is used in various fields like medical, industrial and electronic applications (Esa, Tasirin, & Rahman, 2014). Titanium dioxide is a semiconductor metal oxide used as a photocatalyst for the removal of highly toxic and non-destructive contaminants (Nainani, Thakur, & Chaskar, 2012). As a new antibacterial agent, Ag and titanium dioxide particles have attracted attention in recent years due to good properties such as stability, durability and safety (Sondi & Salopek-Sondi, 2004).

The aim of this study was to find a simple and inexpensive method for monitoring the growth of pathogenic bacteria by constructing a conductometry nanobiosensor using bacterial cellulose/polypyrrole/TiO<sub>2</sub>-Ag. Bacterial cellulose has a porous flexible and structure, functional groups and bio-polymer feature, so it is a good substrate and biodegradable material that can be covered with conductive polymer. Polypyrrole can be synthesized in the BC surface by chemical methods and polypyrrole has good stability (chemical and physical stability) on the BC surface. TiO<sub>2</sub>-Ag nanoparticles as a semiconductor material could enhance electrical conductivity, also these nanoparticles have antibacterial activity that could improve the interaction of PPy sensors with different bacteria. We believe that the higher the electrical conductivity of the film surface and the higher the interaction of the film surface with different bacteria, the greater the sensitivity of the PPy film to the bacteria. The sensor response relies on the reaction between BC/PPy/TiO<sub>2</sub>-Ag film surface and bacteria, which is recorded as an electrical signal. The changes in the electrical resistance of the BC/PPy/TiO<sub>2</sub>-Ag conducting film are measured and is used to calculate the bacteria growth.

## 2. Material and methods

### 2.1. Reagents, chemicals and microorganisms

The BC film was purchased from the Nano-Novin Polymer Co (Sari, Iran). TiO<sub>2</sub>-Ag nanoparticles were purchased from Nano-Gilozak Co (Tehran, Iran). Pyrrole (Fluka, Switzerland) was distilled and stored in a refrigerator in the dark prior to use. Ferric chloride (FeCl<sub>3</sub>) was used as oxidant from Sigma-Aldrich, USA. Some other organic compounds were purchased from Merck. The culture medium, Nutrient broth (Merck, Darmstadt, Germany), was used. *Escherichia coli* PTCC 1330 and *Staphylococcus aureus* PTCC 1112 were purchased from the collection center of industrial microorganisms of Iran, *Aeromonas hydrophyla* ATCC 35654, *Staphylococcus aureus* ATCC 25904, and *Staphylococcus epidermidis* ATCC 700576 were provided from Artemia Research Institute of Urmia University and used for study sensor

**Table 1**

List of experiments in the central composite design (CCD).

Film (Sensor)	Factors	
	A: Pyrrole (mol/L)	B:TiO <sub>2</sub> -Ag (mol/L)
F1 (S1)	0.1	0
F2 (S2)	0.1	0.005
F3 (S3)	0.055	0.005
F4 (S4)	0.055	0.005
F5 (S5)	0.055	0
F6 (S6)	0.055	0.005
F7 (S7)	0.055	0.005
F8 (S8)	0.01	0
F9 (S9)	0.01	0.01
F10 (S10)	0.01	0.005
F11 (S11)	0.055	0.005
F12 (S12)	0.1	0.01
F13 (S13)	0.055	0.01

properties.

### 2.2. Preparation of BC/PPy/TiO<sub>2</sub>-Ag film

#### 2.2.1. BC/PPy/TiO<sub>2</sub>-Ag film synthesis

Chemical polymerization was used to synthesize polypyrrole. In this method, an oxidizing agent (FeCl<sub>3</sub>) was used to initiate the polymerization process. Firstly, to remove impurities, the BC gel membrane was washed with distilled water several times. The 10 × 10 cm piece of BC gel membrane was immersed (according to the experimental design mentioned in Table 1) in 20 ml of solution containing different concentrations of TiO<sub>2</sub>-Ag (0, 0.05 and 0.1 mol/L), pyrrole (0.01, 0.055 and 0.1 mol/L), and TiO<sub>2</sub>-Ag-pyrrole on a polystyrene plate (15 × 15 cm<sup>2</sup>). Afterward, 20 ml of a FeCl<sub>3</sub> solution (0.1 mol/L in the films in which PPy was synthesized) was added to the mentioned solution over 10 min. The synthesis and formation of the films (BC/PPy, BC/TiO<sub>2</sub>-Ag, and BC/PPy/TiO<sub>2</sub>-Ag) were completed according to the experimental design; the films were dried at room temperature under atmospheric conditions for about 24 h. The prepared films were stored in a dark place before use. Fig. 1A shows the BC, BC/TiO<sub>2</sub>-Ag, BC/Py/TiO<sub>2</sub>-Ag, and BC/PPy films.

#### 2.2.2. Characterization study of films

The infrared spectroscopy (Tensor 27, Bruker, Germany) was used to investigate the interactions between TiO<sub>2</sub>-Ag, polypyrrole and cellulose. First, about 2 mg of each film was molded manually, then mixed with KBr (1:100) and pressed to form a tablet with a thickness of about 1 ml. The FT-IR spectroscopy tests were performed in ranging from 4000 to 400 cm<sup>-1</sup> (Amiri, Mokarram, Khiabani, Bari, & Khaledabad, 2019).

To investigate the morphology of films and study their structure, the scanning electron microscope (model Leo 1430 VP, Oberkochen) was used. The images were prepared from the surface of the films. The films were coated with gold before examination, and then figures were prepared (at voltage 15 KV) with different magnifications (Moghanjoui, Bari, Khaledabad, Almasi, & Amiri, 2020).

### 2.3. Cultivating bacteria and preparation of bacterial suspensions

For preparation of bacterial culture, first each bacterium added to 10 ml nutrient broth individually and incubated at 37 °C for 24 h. After that the cultures were subculture in 100 ml nutrient broth at same condition again. The subcultures were centrifugation at 5,000 × g for 15 min at 4 °C to harvest bacterial. Then the pellets were washed twice with sterile normal saline solution and used for preparation bacterial suspensions using McFarland's standards. Barium chloride and sulfuric acid were used to prepare standard McFarland solutions. McFarland solutions were prepared according to the Table 2. Bacterial colonies

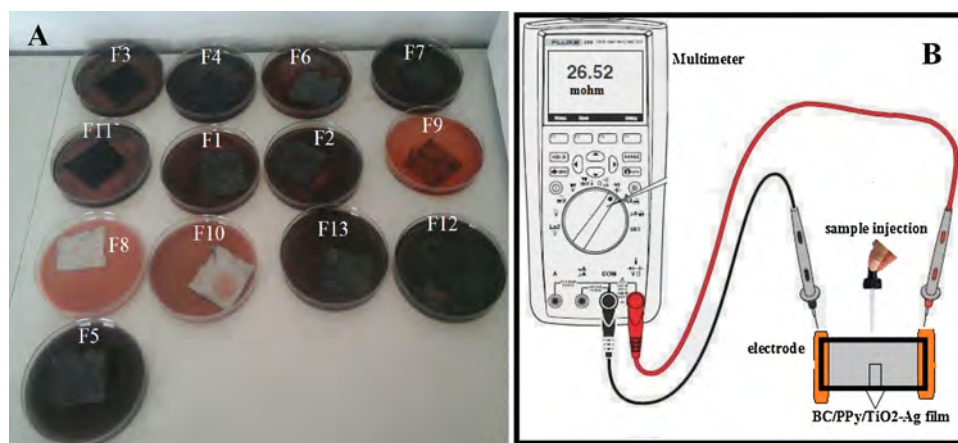


Fig. 1. Different BC, BC/TiO<sub>2</sub>-Ag, BC/PPy and BC/Py/TiO<sub>2</sub>-Ag films (A) and bacteria sample injection system to the sensors (B).

**Table 2**  
McFarland's standard.

Bacteria suspension(CFU/ml)	BaCl <sub>2</sub> (ml)	Sulfuric acid (ml)	McFarland's standard
$1.5 \times 10^8$	0.05	9.95	0.5
$310^8$	0.10	9.90	1
$6 \times 10^8$	0.20	9.80	2
$9 \times 10^8$	0.30	9.70	3
$1.2 \times 10^9$	0.40	9.60	4

were taken by sterilizing loops and distributed into test tubes containing sterile normal saline solution. Bacterial suspensions were prepared according to McFarland standards (0.5, 1, 2, 3, and 4). The turbidity of suspensions was measured by spectrophotometer at 625 nm, which was 0.910, 0.250, 0.423, 0.550, and 0.650, respectively. The microbial load of the suspensions is equal to McFarland's standard. How to prepare McFarland standard solutions and the amount of microbial load of suspensions are given in Table 2. Finally, bacterial suspensions were centrifuged at  $5,000 \times g$  for 15 min at 4 °C and the bacterial cells were washed three times with sterile normal saline solution.

#### 2.4. Design BC/PPy/TiO<sub>2</sub>-Ag sensor and study sensory properties

The BC/PPy/TiO<sub>2</sub>-Ag sensor consisting of a film of  $2 \times 1$  cm dimension having a thickness of 0.5 mm was put in a glass plate. The both ends of a BC/PPy/TiO<sub>2</sub>-Ag sensor were connected to the multimeter by copper wires. The BC/PPy/TiO<sub>2</sub>-Ag film's resistance change was tested with centrifuged bacterial suspensions (Fig. 1B) system. Centrifuged bacteria (1  $\mu$ l) were transferred to the BC/PPy/TiO<sub>2</sub>-Ag film surface and electrical resistance changes were recorded. In the next step, the different concentrations of the bacteria were added to the film surface and the resistance changes were recorded (R). It should be mentioned that before the transfer of bacteria, the electrical resistance of the nanocomposites was measured by the multimeter system ( $R_0$ ). The signal resulting from a sensor–bacteria interaction is quantified in terms of the relative electrical resistance difference (RRD) of the film used as sensor. The RRD was calculated by  $(R-R_0)/R_0$ , where  $R_0$  and R denote the initial resistance and real-time resistance (resistance of the sensor when it was exposed to bacteria). The RRDs of the sensors were measured after several second of exposure to each bacterium (for three replicate injections).

#### 2.5. Statistical analysis

In this study, CCD was used to study the effect of two variables, including pyrrole concentration and TiO<sub>2</sub>-Ag concentration in the

sensor's properties (detection limit, regression coefficient, sensitivity and linear range). Based on this design, 13 sensors were designed and tested. The Design-Expert 7 software (Statease Inc., Minneapolis, USA) was also used to analyze the effects of pyrrole and TiO<sub>2</sub>-Ag concentrations and plotting the graphs, and Excel 2016 software was used to calculate the figure of merits of the sensors. Also, significant levels of data were considered at the 5 % probability level ( $P < 0.05$ ). Table 1 shows the list of sensors made based on the concentration of pyrrole and TiO<sub>2</sub>-Ag.

### 3. Result and discussion

#### 3.1. Study morphology of synthesized films using SEM

In order to determine the size and morphology of BC/PPy/TiO<sub>2</sub>-Ag films, SEM images were obtained from the film surface. Fig. 2 shows the SEM film of pure BC (A), BC/PPy (B), BC/TiO<sub>2</sub>-Ag (C), BC/PPy/TiO<sub>2</sub>-Ag (D) and TiO<sub>2</sub>-Ag powder (E) films in different magnifications. As shown in Fig. 2A, the pure BC had porous-hydrogel shape. Comparison of microscopic images of pure bacterial cellulose fibers with polypyrrole coated fibers revealed that polypyrrole had covered bacterial cellulose fibers (Wang et al., 2013). The PPy particles were observed like a thin shell that had blocked the bacterial cellulose fibers. After polymerization of polypyrrole nanoparticles, they were placed on the surface of bacterial cellulose (Fig. 2B). Hydrogen bonds between the polypyrrole amine groups and the bacterial cellulose hydroxyl group may act as a tensile force to help bond polypyrrole and cellulose nanoparticles (Peng et al., 2016). As shown in Fig. 2C, cellulose nanoparticles were covered with TiO<sub>2</sub>-Ag nanoparticles. Most of these nanoparticles are irregular and spherical in size from 50 to 90 nm, which are distributed on the cellulose surface. In Fig. 2D, it was observed that with the addition of PPy and TiO<sub>2</sub>-Ag to cellulose film, its density decreased and a porous network with cavities and cracks was observed. The Fig. 2E is related to the TiO<sub>2</sub> nanoparticle embedded with silver. According to the image of the particles, they are spherical and approximately uniform in size of 80 nm. In the sample, the amount of particle aggregation is observed, which is probably due to the presence of silver particles.

#### 3.2. Study structure of synthesized films using FT-IR

In order to ensure the presence of TiO<sub>2</sub>-Ag nanoparticles and confirm the binding between bacterial cellulose and PPy and TiO<sub>2</sub>-Ag, FT-IR test was carried out. Fig. 3 shows FT-IR spectra of BC/TiO<sub>2</sub>-Ag (A), BC/PPy (B), BC/PPy/TiO<sub>2</sub>-Ag (C), pure BC (D) and pure TiO<sub>2</sub>-Ag (E). In the spectra of BC/TiO<sub>2</sub>-Ag (Fig. 3A) the peak at  $664 \text{ cm}^{-1}$  is dedicated to the Ti–O–Ti elongation. The peak at  $1012 \text{ cm}^{-1}$  corresponds to a specific O–O tensile vibration. The sharp peak at  $1400 \text{ cm}^{-1}$  is

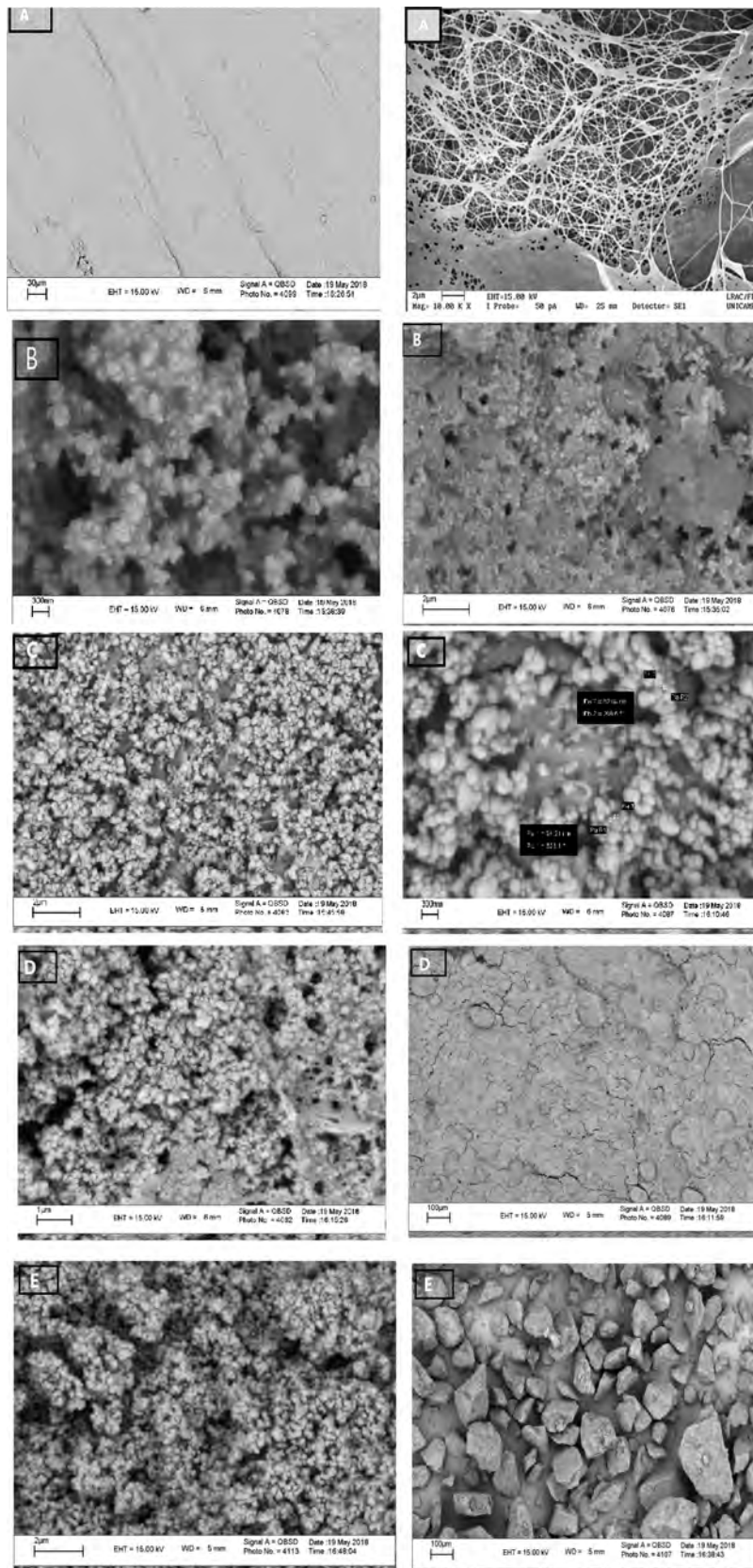


Fig. 2. SEM images of pure BC (A), BC/PPy (B), BC/TiO<sub>2</sub>-Ag (C), BC/PPy-TiO<sub>2</sub>-Ag (D) films and TiO<sub>2</sub>-Ag powder (E).

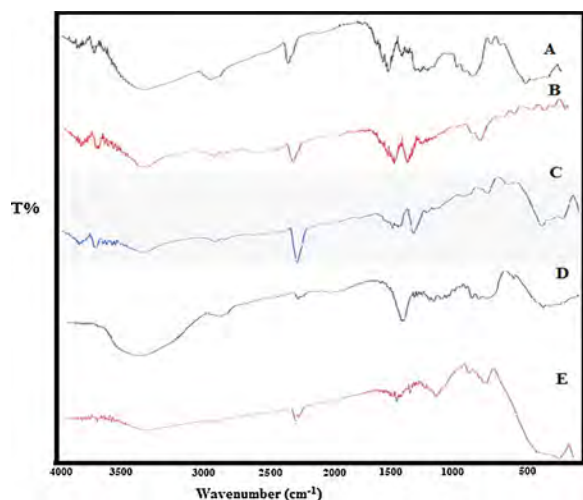


Fig. 3. FT-IR spectra of BC/TiO<sub>2</sub>-Ag (A), BC/PPy (B), BC/PPy/TiO<sub>2</sub>-Ag (C), pure BC (D), and pure TiO<sub>2</sub>-Ag (E).

probably related to TiO<sub>2</sub> network vibrations (Cui, Yang, Wang, & Wang, 2016). In the BC/PPy spectra (Fig. 3B) the peak at 1525 cm<sup>-1</sup> is related to the tensile vibration of the C=C bond in the pyrrole ring. The peak at 1470 cm<sup>-1</sup> refers to the tensile vibration of the C-N bond in the pyrrole ring. The peaks at 1300 cm<sup>-1</sup> is also related to the vibration of the C-H bond and the peak at 1250 cm<sup>-1</sup> is related to the pyrrole ring vibrations. According to the results of this test, it can be stated that pyrrole synthesis has been successfully performed (Wang et al., 2013).

In the BC/PPy-TiO<sub>2</sub>-Ag spectra (Fig. 3C) the peaks at 796 cm<sup>-1</sup> and 930 cm<sup>-1</sup> are related to the C-H bond. The peaks at 1197 cm<sup>-1</sup> is

related to the relationship between N-C and N-C tensile bonding (Cui et al., 2016). The peaks at 1470 cm<sup>-1</sup> and 1563 cm<sup>-1</sup> are related to the vibration of the pyrrole ring (Cui et al., 2016). A short peak in the range of 3000–3500 cm<sup>-1</sup> may be related to the elongation of the N-H bonds. These results show a strong interaction between polypyrrole and TiO<sub>2</sub>-Ag (Cui et al., 2016). In the pure BC spectra (Fig. 3D) the peak in 3350 cm<sup>-1</sup> is attributed to the tensile vibrations of hydroxyl and peak groups at 12900 cm<sup>-1</sup> are related to the tensile vibrations of C-H carbohydrates. The 1159 cm<sup>-1</sup> peak corresponds to the asymmetric tensile bonding of the C-O. The peak at 1050 cm<sup>-1</sup> is attributed to hydroxyl and C-O-C groups and tensile vibrations of carbohydrates (Liang et al., 2015). The peaks at 1427, 1314 and 1031 cm<sup>-1</sup> are due to C-C vibration. In the pure TiO<sub>2</sub>-Ag spectra (Fig. 3E) the peaks related to the tensile vibration of OH are observed in the range of 2850–3428 cm<sup>-1</sup> (Bae & Choi, 2003) and the broad peak observed at 400 cm<sup>-1</sup> are related to Ti-O-Ti bond vibrations (Yan, He, Evans, Zhu, & Duan, 2004). The tensile vibrations of the hydroxyl group are observed in the region of 3415 cm<sup>-1</sup> and the tensile vibration of carbon-hydrogen in the region of 2920 cm<sup>-1</sup>, the flexural vibrations of the hydroxyl group in the region of 1445 cm<sup>-1</sup> and the tensile vibrations of Ti=O are observed in the 1119 cm<sup>-1</sup> region.

By comparing the pure BC spectrum with BC/TiO<sub>2</sub>-Ag, it is clear that the peaks of 891 cm<sup>-1</sup> and 940 cm<sup>-1</sup>, which are present in pure TiO<sub>2</sub>-Ag, is also observed in BC/TiO<sub>2</sub>-Ag nanocomposite, which indicates that the proper physical bonding between the TiO<sub>2</sub>-Ag and the cellulose is created. By comparing the pure BC spectrum with BC/PPy, a peak was created in the 13750 cm<sup>-1</sup> region, indicating the formation of physical bonds between bacterial cellulose and polypyrrole. By comparing the spectra of films containing polypyrrole with polypyrrole-free films, it is clear that in films containing the PPy (BC/PPy and BC/PPy/TiO<sub>2</sub>-Ag) the peak at 2800 cm<sup>-1</sup> was deleted, which indicates a strong

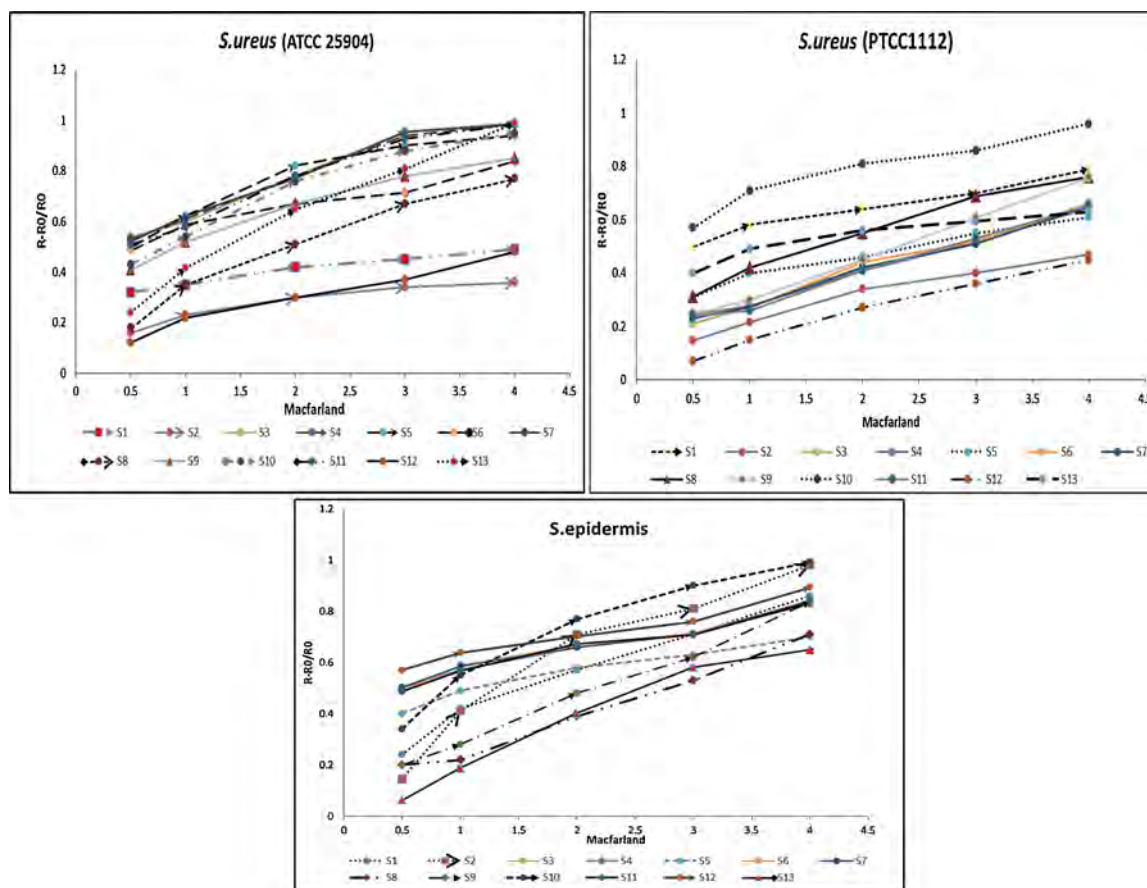


Fig. 4. Response curve of sensors to Gram-positive bacteria.

**Table 3**  
Figure of merit of sensors to Gram-positive bacteria.

Sensor	<i>S. aureus</i> ATCC 25904				<i>S. epidermidis</i> ATCC 700576				<i>S. aureus</i> PTCC 1112			
	DL	LR	Sensitivity	R <sup>2</sup>	DL	LR	Sensitivity	R <sup>2</sup>	DL	LR	Sensitivity	R <sup>2</sup>
1	0.5	0.5-4	0.0484	0.9747	0.5	0.5-4	0.1671	0.9757	0.5	0.5-4	0.0604	0.979
2	0.5	0.5-4	0.055	0.9093	0.5	0.5-4	0.224	0.9287	0.5	0.5-4	0.0911	0.971
3	0.5	0.5-4	0.1387	0.9597	0.5	0.5-4	0.0901	0.9783	0.5	0.5-4	0.1263	0.993
4	0.5	0.5-4	0.1381	0.9589	0.5	0.5-4	0.0876	0.9842	0.5	0.5-4	0.1381	0.958
5	0.5	0.5-4	0.1259	0.91	0.5	0.5-4	0.0805	0.9589	0.5	0.5-4	0.0820	0.974
6	0.5	0.5-4	0.1395	0.9596	0.5	0.5-4	0.091	0.9645	0.5	0.5-4	0.1202	0.987
7	0.5	0.5-4	0.1366	0.9665	0.5	0.5-4	0.0881	0.9715	0.5	0.5-4	0.1233	0.994
8	0.5	0.5-4	0.1637	0.9687	0.5	0.5-4	0.1494	0.9892	0.5	0.5-4	0.1283	0.977
9	0.5	0.5-4	0.1246	0.967	0.5	0.5-4	0.1802	0.9958	0.5	0.5-4	0.1458	0.997
10	0.5	0.5-4	0.1511	0.9538	0.5	0.5-4	0.1791	0.9339	0.5	0.5-4	0.1005	0.933
11	0.5	0.5-4	0.1439	0.967	0.5	0.5-4	0.0912	0.9697	0.5	0.5-4	0.1232	0.992
12	0.5	0.5-4	0.0952	0.9777	0.5	0.5-4	0.085	0.9735	0.5	0.5-4	0.1067	0.989
13	0.5	0.5-4	0.2075	0.9829	0.5	0.5-4	0.1719	0.9667	0.5	0.5-4	0.0762	0.912

interaction between bacterial cellulose and polypyrrole. By comparing the FTIR spectrum of pure BC and pure TiO<sub>2</sub>-Ag with its composite state (BC/PPy, BC/TiO<sub>2</sub>-Ag and BC/PPy/TiO<sub>2</sub>-Ag), it is observed that the peaks related to the pure state of these compounds in composite state have been transferred to a shorter or larger wavenumbers that indicates the creation of electrostatic forces between cellulose and polypyrrole and TiO<sub>2</sub>-Ag.

### 3.3. Evaluation of response of sensors to bacteria

#### 3.3.1. Evaluation of response of sensors to Gram-positive bacteria

Fig. 4 and Table 3 show the response curve and figure of merits of the sensors to the Gram-positive bacteria. After plotting the response curves of the sensors to the bacteria, the electrical resistance changes were considered as sensitivity. Also, the regression coefficient (R<sup>2</sup>) and the linear range (LR) of the curves based on McFarland were calculated.

The detection limit (DL) of the sensors based on McFarland, was calculated as follows:

$$DL = \frac{3\sigma_b}{\text{Calibration sensitivity}}$$

Where  $3\sigma_b$  is standard deviation of blank and calibration sensitivity is the slope of curve of (R-R<sub>0</sub>/R<sub>0</sub>) Vs Macfarland. The dimension of calibration sensitivity is 1/McFarland.

The results showed that among sensors, sensitivity of S13 to *S. aureus* ATCC 25904 was more than other sensors. This sensor had a mean concentration of polypyrrole (0.055 M) and a maximum concentration of TiO<sub>2</sub>-Ag (0.01). The S1 also had the lowest sensitivity to *S. aureus* ATCC 25904. This sensor has the highest pyrrole concentration (0.1) and does not contain TiO<sub>2</sub>-Ag. The results showed that in the sensors with the same pyrrole concentrations and different TiO<sub>2</sub>-Ag concentration, by increasing TiO<sub>2</sub>-Ag concentration the sensitivity were

increased, which may be due to the conductivity of these nanoparticles. Sensitivity of S2 to *S. epidermidis* ATCC 700576 was higher than other sensors. This sensor had the highest concentration of polypyrrole and a moderate amount of TiO<sub>2</sub>-Ag. Sensitivity of S5 to *S. epidermidis* ATCC 700576 bacteria was also lower than other sensors. This sensor had a moderate concentration of PPy and did not contain TiO<sub>2</sub>-Ag. S9 had the highest sensitivity to *S. aureus* PTCC 1112. This sensor had the lowest concentration of polypyrrole and the highest amount of TiO<sub>2</sub>-Ag. S1 had the least sensitivity to *S. aureus* PTCC 1112. This sensor had the highest PPy concentration and did not contain TiO<sub>2</sub>-Ag. Among the Gram-positive bacteria, S1, S2, S9, and S10 showed the highest sensitivity to *S. epidermidis* ATCC 700576, and S3, S4, S5, S6, S7, S8, S11, S12 and S13 showed a high sensitivity to *S. aureus*. The reason for the better response of sensors in the presence of *S. aureus* in compare to *S. epidermidis* ATCC 700576 bacteria may be due to the presence of biofilm with a negative charge on the cell wall of *S. aureus*. Biofilm is a complex microbial community that is created by secretion of a matrix (proteins, DNA, and polysaccharides) and captures the bacterial cell's community. Important noteworthy is that the formation of biofilm protects the pathogenic bacteria against antibiotics and is one of the main causes of the development of chronic infections. The electrostatic properties of nanoparticles and microbial biofilm influence their interactions. In most bacteria, the biofilm matrix has a negative charge, but *S. epidermidis* forms a poly-cationic biofilm (Landini, Antoniani, Burgess, & Nijland, 2010). Pirsra and co-workers reported that the polypyrrole based sensor showed high sensitivity toward compounds with high electron donor ability like NH<sub>3</sub> and amines that confirms the results of this study (Alizadeh, Pirsra, Mani-Varnosfaderani, & Alizadeh, 2015; Pirsra, Shamusi, & Kia, 2018; Pirsra, Zandi, Almasi, & Hasanlu, 2015).

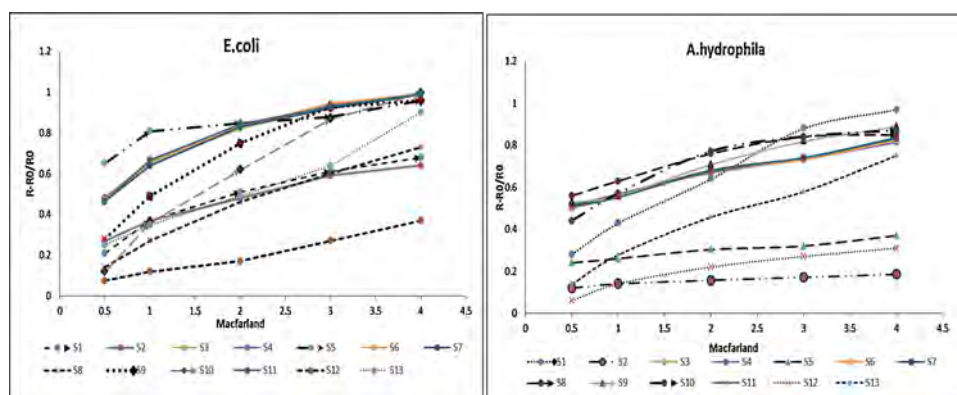


Fig. 5. Response curve of sensors to Gram-negative bacteria.

**Table 4**  
Figure of merits of sensors to Gram-negative bacteria.

Sensor	<i>E. coli</i> PTCC 1330				<i>A. hydrophyla</i> ATCC 35654			
	DL	LR	Sensitivity	R <sup>2</sup>	DL	LR	Sensitivity	R <sup>2</sup>
1	0.5	0.5-4	0.1277	0.936	0.5	0.5-4	0.201	0.975
2	0.5	0.5-4	0.1049	0.965	0.5	0.5-4	0.117	0.965
3	0.5	0.5-4	0.1428	0.922	0.5	0.5-4	0.092	0.985
4	0.5	0.5-4	0.1405	0.914	0.5	0.5-4	0.085	0.991
5	0.5	0.5-4	0.0732	0.934	0.5	0.5-4	0.035	0.981
6	0.5	0.5-4	0.1429	0.914	0.5	0.5-4	0.088	0.987
7	0.5	0.5-4	0.1437	0.916	0.5	0.5-4	0.091	0.988
8	0.5	0.5-4	0.1659	0.985	0.5	0.5-4	0.086	0.917
9	0.5	0.5-4	0.195	0.912	0.5	0.5-4	0.109	0.983
10	0.5	0.5-4	0.247	0.966	0.5	0.5-4	0.122	0.916
11	0.5	0.5-4	0.141	0.913	0.5	0.5-4	0.094	0.990
12	0.5	0.5-4	0.082	0.985	0.5	0.5-4	0.068	0.942
13	0.5	0.5-4	0.177	0.983	0.5	0.5-4	0.167	0.987

### 3.3.2. Evaluation of response of sensors to Gram-negative bacteria

Fig. 5 and Table 4 show the response curve and figure of merit of the sensors to the Gram-negative bacteria. Results showed that S10 was more sensitive to *E. coli* PTCC 1330 than other sensors. This sensor had the lowest concentration of polypyrrole and the average concentration of TiO<sub>2</sub>-Ag. S5 also had the least sensitivity to this *E. coli* PTCC 1330. This sensor had a high concentration of polypyrrole and no TiO<sub>2</sub>-Ag nanoparticles. Also, S1 was more sensitive to *A. hydrophyla* ATCC 35654 than other sensors. This sensor had the highest concentration of polypyrrole and did not contain TiO<sub>2</sub>-Ag nanoparticles. S5 also had the least sensitivity to *A. hydrophyla* ATCC 35654. This sensor had an average concentration of PPy and no TiO<sub>2</sub>-Ag nanoparticles. Among the two Gram-negative bacteria, sensitivity of all sensors to *E. coli* PTCC 1330 was significantly higher than *A. hydrophyla* ATCC 35654. This result may be due to this fact that *E. coli* had a larger size than *A. hydrophyla*, so *E. coli* had large cell wall size and greater electrical charge that affects the sensor electrical resistance. Shen, Tan, Xu, Xu and Yao (2013) used impedance-based technology to measure the concentration of bacterial suspensions. In this experiment, the electrical conductivity of *Bacillus subtilis*, *Pseudomonas fluorescens* and *E. coli* was measured. According to the results, in the study, Gram-negative bacteria of *P. fluorescens* and *E. coli* had similar conduction curves, and the curvature of these two gram-negative bacteria were linear than the Gram-positive bacteria curve. While the *B. subtilis* strain curve was different from Gram-negative bacteria. They reported that this difference may be related to the difference in membrane and cell wall of these bacteria. The results obtained in our research were consistent with their results. In other studies, Carstensen, Marquis, Child and Bender (1979) and Yang, Lin, Wei, Wu and Lin (2003) reported that changes in electrical conductivity were related to the surface electrical charge of bacterial and lipid membrane of bacteria. Phosphatidylglycerol, phospholipid hydroxylate, Cardiolipin and phosphatidylserine, which are components of the outer membrane of the bacteria, are negatively charged. Van der Wal, Minor, Norde, Zehnder and Lyklema (1997) reported that the surface of bacterial cells had a negative charge due to the presence of phosphoryl ionized and carboxylates in the outer membrane. In the present study, the sensors were sensitive to Gram-negative bacteria more than Gram-positive bacteria, because Gram-negative bacteria had a higher negative charge on their surface. It should be mentioned that bacteria that have a larger size and larger surface electrical charge have a greater effect on the sensors. So our results are consistent with the results of reported research.

### 3.4. Study simultaneous effect of pyrrole and TiO<sub>2</sub>-Ag concentration on the sensitivity of sensors to bacteria based RSM

Fig. 6 shows 3-D plots of the effect of the concentration of pyrrole and TiO<sub>2</sub>-Ag on the sensitivity of the sensors to different bacteria.

According to the results, there was a significant difference between the response of the sensors to the *S. aureus* ATCC 25904 ( $P < 0.05$ ). Sensitivity of sensors to the *S. aureus* ATCC 25904 bacterium was increased by increasing the pyrrole concentration to an average of (0.055 M) but at the higher concentration the sensitivity of the sensors was decreased. Therefore, it can be concluded that the pyrrole at moderate concentration has a positive effect on conductivity and increases the sensitivity, but more concentration of pyrrole causes antimicrobial activity of sensor that causes a decrease in sensitivity of the sensors. The sensitivity of the bacteria has also increased with increasing the amount of TiO<sub>2</sub>-Ag nanoparticles. Also results showed that pyrrole and TiO<sub>2</sub>-Ag concentration had a significant effect on the sensor sensitivity to *A. hydrophyla* ATCC 35654 ( $P < 0.05$ ). By increasing the concentration of pyrrole and TiO<sub>2</sub>-Ag, the sensitivity of the sensors to this bacterium had increased. As shown in the figures, Pyrrole and TiO<sub>2</sub>-Ag had no significant effect on the sensitivity of the sensors to *S. aureus* PTCC 1112 and *S. epidermidis* ATCC 700576. According to the 3-D plots, changes in the concentration of Pyrrole and TiO<sub>2</sub>-Ag had a significant effect on the sensors response to *E. coli* PTCC 1330 ( $P < 0.05$ ). The amount of TiO<sub>2</sub>-Ag had a greater effect on sensor sensitivity than pyrrole. Increasing the amount of TiO<sub>2</sub>-Ag increased the sensitivity of sensors to the *E. coli* PTCC 1330, while the sensitivity of sensors to *E. coli* PTCC 1330 was low at a maximum pyrrole concentration. The reason for the decrease in sensitivity in the high concentration of Pyrrole may be due to this fact that the pyrrole at high concentration covers the surface of the cellulose film and does not allow to bacteria to bind to the sensor surface so interaction between bacteria and sensor surface is decreased.

There are several theories to interpret the sensing mechanism of conducting polymer. Doping and undoping play key roles in the sensing mechanism of conducting polymer based sensors. Their doping level can be altered by transferring electrons from or to the analytes. Electron transferring can cause the changes in resistance and work function of the sensing material. This process occurred when PPy or other conducting films exposed in  $\sigma$ - and  $\pi$ -electron donor materials (Pirsa & Alizadeh, 2010). When this occurs at a p-type conducting polymer, the doping level as well as the electric conductance of the conducting polymer is enhanced. BC/PPy/TiO<sub>2</sub>-Ag behaves like p-type semiconductors via appropriate doping and can arouse the change of conductivity through interaction with bacteria (Pirsa & Alizadeh, 2010; Pirsa et al., 2015). The mechanism of antibacterial activity of TiO<sub>2</sub>-Ag is based on the production of reactive oxygen by silver, this mechanism applies more to nanosilver composites that are placed on semiconductor bases such as TiO<sub>2</sub>. In this situation, the particle acts as an electrochemical cell and by oxidizing the oxygen atom, producing the oxygen ion and by hydrolyzing the water, it produces OH<sup>-</sup> ions, both of which are active and strong antimicrobial agents. So when bacteria interact with BC/PPy/TiO<sub>2</sub>-Ag film, these ions can be created and change electrical conductivity of BC/PPy/TiO<sub>2</sub>-Ag film.

## 4. Conclusion

In this study, new sensors based on BC/PPy/TiO<sub>2</sub>-Ag were provided for rapid and easy detection of bacteria growth in food samples. The BC/PPy/TiO<sub>2</sub>-Ag nanocomposite was synthesized in 13 formulations. Then, 5 bacteria including *E. coli* PTCC 1330, *S. aureus* ATCC25904, *S. aureus* PTCC 1112, *S. epidermidis* ATCC 700576, and *A. hydrophyla* ATCC 35654 were added to the sensor films and the electrical resistance changes were measured by the multimeter (as sensors response). According to the results in sensors with high Pyrrole concentration, high electrical conductivity and high sensitivity were observed. In general, the sensors responded to Gram-negative bacteria better than Gram-positive. The nanoparticles used in making sensors (PPy and TiO<sub>2</sub>-Ag) have a positive charge. If the tested bacterium has a negative charge, the response of the sensor to the bacteria will be greater. The response of the sensors to the bacteria is also affected by the size and the environment of the bacterial cell. The TiO<sub>2</sub>-Ag nanoparticles

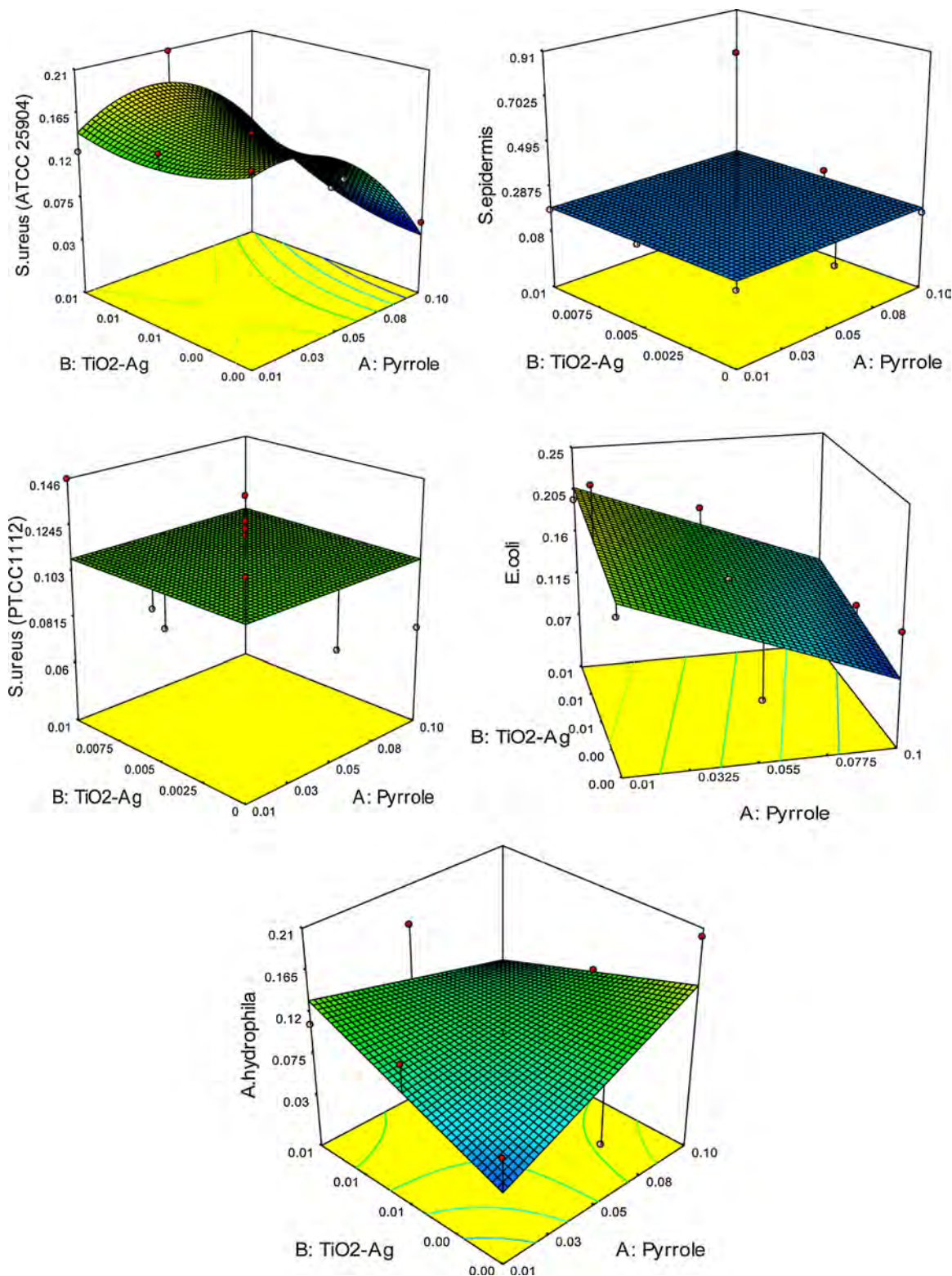


Fig. 6. 3-D plots of effect of Pyrrole and TiO<sub>2</sub>-Ag on the sensitivity of sensors to different bacteria.

showed little antimicrobial activity on bacteria and had little effect on the response of the sensors. But these nanoparticles had positive electrical charge and conductivity, so could increase the sensitivity of the sensors. The advantage of the fabricated biosensor in this work is that it can be used anywhere. These biosensors are portable, their synthesis is easy, easy to use and does not require skilled operators, and the response time of these sensors is very short for target analysis and is very

sensitive. Therefore, they have the potential to use as diagnostic tools to improve biological safety.

#### Acknowledgements

The financial support of the Research Council of Urmia University is gratefully acknowledged.

## References

- Alizadeh, N., Pirs, S., Mani-Varnosfaderani, A., & Alizadeh, M. S. (2015). Design and fabrication of open-tubular array gas sensors based on conducting polypyrrole modified with crown ethers for simultaneous determination of alkylamines. *IEEE Sensors Journal*, 15(7), 4130–4136.
- Amiri, S., Mokarram, R. R., Khiabani, M. S., Bari, M. R., & Khaledabad, M. A. (2019). Exopolysaccharides production by *Lactobacillus acidophilus* LA5 and *Bifidobacterium animalis* subsp. *lactis* BB12: Optimization of fermentation variables and characterization of structure and bioactivities. *International Journal of Biological Macromolecules*, 123, 752–765.
- Bae, E., & Choi, W. (2003). Highly enhanced photoreductive degradation of per-chlorinated compounds on dye-sensitized metal/TiO<sub>2</sub> under visible light. *Environmental Science & Technology*, 37(1), 147–152.
- Carstensen, E. L., Marquis, R. E., Child, S. Z., & Bender, G. R. (1979). Dielectric properties of native and deoated spores of *Bacillus megaterium*. *Journal of Bacteriology*, 140(3), 917–928.
- Cui, S., Yang, L., Wang, J., & Wang, X. (2016). Fabrication of a sensitive gas sensor based on PPy/TiO<sub>2</sub> nanocomposites films by layer-by-layer self-assembly and its application in food storage. *Sensors and Actuators B: Chemical*, 233, 337–346.
- DaSilva, J. S., Oliveira, M. D., de Melo, C. P., & Andrade, C. A. (2014). Impedimetric sensor of bacterial toxins based on mixed (Concanavalin A)/polyaniline films. *Colloids and Surfaces B: Biointerfaces*, 117, 549–554.
- Detsri, E., & Popanyasak, J. (2015). Fabrication of silver nanoparticles/polyaniline composite thin films using layer-by-layer self-assembly technique for ammonia sensing. *Colloids and Surfaces A, Physicochemical and Engineering Aspects*, 467, 57–65.
- Esa, F., Tasirin, S. M., & Rahman, N. A. (2014). Overview of bacterial cellulose production and application. *Agriculture and Agricultural Science Procedia*, 2, 113–119.
- Hamada, R., Takayama, H., Shonishi, Y., Mao, L., Nakano, M., & Suehiro, J. (2013). A rapid bacteria detection technique utilizing impedance measurement combined with positive and negative dielectrophoresis. *Sensors and Actuators B: Chemical*, 181, 439–445.
- Hiremath, N., Guntupalli, R., Vodyanoy, V., Chin, B. A., & Park, M. K. (2015). Detection of methicillin-resistant *Staphylococcus aureus* using novel lytic phage-based magnetoelastic biosensors. *Sensors and Actuators B: Chemical*, 210, 129–136.
- Landini, P., Antoniani, D., Burgess, J. G., & Nijland, R. (2010). Molecular mechanisms of compounds affecting bacterial biofilm formation and dispersal. *Applied Microbiology and Biotechnology*, 86(3), 813–823.
- Lei, Y., Chen, W., & Mulchandani, A. (2006). Microbial biosensors. *Analytica Chimica Acta*, 568(1–2), 200–210.
- Liang, B., Qin, Z., Li, T., Dou, Z., Zeng, F., Cai, Y., et al. (2015). Poly (aniline-co pyrrole) on the surface of reduced graphene oxide as high-performance electrode materials for supercapacitors. *Electrochimica Acta*, 177, 335–342.
- Luong, J. H. T., Mulchandani, A., & Guilbault, G. G. (1988). Developments and applications of biosensors. *Trends in Biotechnology*, 6(12), 310–316.
- Moghanjoui, Z. M., Bari, M. R., Khaledabad, M. A., Almasi, H., & Amiri, S. (2020). Bio-preservation of white brined cheese (Feta) by using probiotic bacteria immobilized in bacterial cellulose: Optimization by response surface method and characterization. *LWT*, 117, 108603.
- Nainani, R., Thakur, P., & Chaskar, M. (2012). Synthesis of silver doped TiO<sub>2</sub> nanoparticles for the improved photocatalytic degradation of methyl orange. *Journal of Materials Science and Engineering B*, 2(1), 52–58.
- Panfili, G., Manzi, P., Compagnone, D., Scarciglia, L., & Palleschi, G. (2000). Rapid assay of choline in foods using microwave hydrolysis and a choline biosensor. *Journal of Agricultural and Food Chemistry*, 48(8), 3403–3407.
- Peng, S., Fan, L., Wei, C., Bao, H., Zhang, H., Xu, W., et al. (2016). Polypyrrole/nickel sulfide/bacterial cellulose nanofibrous composite membranes for flexible super-capacitor electrodes. *Cellulose*, 23(4), 2639–2651.
- Pirs, S., & Alizadeh, N. (2010). Design and fabrication of gas sensor based on nano-structure conductive polypyrrole for determination of volatile organic solvents. *Sensors and Actuators B: Chemical*, 147(2), 461–466.
- Pirs, S., Shamsi, T., & Kia, E. M. (2018). Smart films based on bacterial cellulose nanofibers modified by conductive polypyrrole and zinc oxide nanoparticles. *Journal of Applied Polymer Science*, 135(34), 46617.
- Pirs, S., Zandi, M., Almasi, H., & Hasanlu, S. (2015). Selective hydrogen peroxide gas sensor based on nanosized polypyrrole modified by CuO nanoparticles. *Sensor Letters*, 13(7), 578–583.
- Shen, F., Tan, M., Xu, H., Xu, Z., & Yao, M. (2013). Development of a novel conductance-based technology for environmental bacterial sensing. *Chinese Science Bulletin*, 58(4–5), 440–448.
- Sondi, I., & Salopek-Sondi, B. (2004). Silver nanoparticles as antimicrobial agent: A case study on *E. Coli* as a model for Gram-negative bacteria. *Journal of Colloid and Interface Science*, 275(1), 177–182.
- Van der Wal, A., Minor, M., Norde, W., Zehnder, A. J., & Lyklema, J. (1997). Conductivity and dielectric dispersion of Gram-positive bacterial cells. *Journal of Colloid and Interface Science*, 186(1), 71–79.
- Wan, Y., Sun, Y., Qi, P., Wang, P., & Zhang, D. (2014). Quaternized magnetic nanoparticles-fluorescent polymer system for detection and identification of bacteria. *Biosensors & Bioelectronics*, 55, 289–293.
- Wang, J., Liu, W., Li, H., Wang, H., Wang, Z., Zhou, W., et al. (2013). Preparation of cellulose fiber-TiO<sub>2</sub> nanobelt-silver nanoparticle hierarchically structured hybrid paper and its photocatalytic and antibacterial properties. *Chemical Engineering Journal*, 228, 272–280.
- Wang, Y., & Alocilja, E. C. (2015). Gold nanoparticle-labeled biosensor for rapid and sensitive detection of bacterial pathogens. *Journal of Biological Engineering*, 9(1), 16.
- Yan, X., He, J., Evans, D. G., Zhu, Y., & Duan, X. (2004). Preparation, characterization and photocatalytic activity of TiO<sub>2</sub> formed from a mesoporous precursor. *Journal of Porous Materials*, 11(3), 131–139.
- Yang, L., & Bashir, R. (2008). Electrical/electrochemical impedance for rapid detection of foodborne pathogenic bacteria. *Biotechnology Advances*, 26(2), 135–150.
- Yang, T. Y., Lin, H. M., Wei, B. Y., Wu, C. Y., & Lin, C. K. (2003). UV enhancement of the gas sensing properties of nano-TiO<sub>2</sub>. *Rev. Adv. Mater. Sci.*, 4(1), 48–54.
- Yoo, S. M., Kim, D. K., & Lee, S. Y. (2015). Aptamer-functionalized localized surface plasmon resonance sensor for the multiplexed detection of different bacterial species. *Talanta*, 132, 112–117.